J MATER RES TECHNOL. 2019;xxx(xx):xxx–xxx

Available online at www.sciencedirect.com

jmr&t Journal of Materials Research and Technology

www.jmrt.com.br

Original Article

Computation-assisted analyzing and forecasting on impurities removal behavior during zone refining of antimony

Xiaoxin Zhang[a,†], *Semiramis Friedrich*[a,*,†], *Bin Liu*[a], *Tianxiang Huang*[b], *Bernd Friedrich*[a]

[a] *IME Process Metallurgy and Metal Recycling, RWTH Aachen University, 52056 Aachen, Germany*

[b] *SLA Institute of Structural Mechanics and Lightweight Design, RWTH Aachen University, 52062 Aachen, Germany*

ARTICLE INFO

Article history:
Received 1 July 2019
Accepted 19 November 2019
Available online xxx

Keywords:
Antimony
Zone refining
Spim-model
Effective distribution coefficient
High purity metal

ABSTRACT

High purity antimony (Sb) gains nowadays a rising interest for high-tech applications. Zone refining is commonly used as a reliable final purification step to achieve higher purity levels of Sb. However, the removal of arsenic (As) - the most troublesome impurity in Sb often occurring in quite high amounts - stays as the challenge during zone refining, due to its very unfavorable distribution coefficient. In addition, there are two important factors, essential to predict the zone refining efficiency and the required time (required number of passes and heater movement velocity), which are still seldom explored. These factors are first the effective distribution coefficient (k_{eff}) and second the ratio of the diffusion layer thickness to the diffusion constant of each impurity (δ/D). Therefore, in the present work, these two research-demanding aspects have been investigated. Firstly, the possibility of removing vaporized As through introducing an inert carrying gas flux was studied by testing two different initial concentrations of As (670 and 430 ppm) and undergoing different process parameters. Higher initial concentrations of As showed to be slightly (10 %) reduced when the melting time increases. Lower As concentration, however, remains almost stable. On the other hand, using the so-called Spim-model, zone refining of Sb was conducted under 1 L/min Nitrogen gas flux at different heater moving velocities (2, 1 and 0.5 mm/min) to calculate the k_{eff} of impurities, derived by fitting the experimental impurity distribution with the simulated profiles. Finally and with the known values of k_{eff}, the values of δ/D for each impurity could be then retrieved by applying the BPS model. That not only allows predicting k_{eff} for any moving velocity based on Spim-model, but also provides an alternative way to calculate these two values when one of them was obtained from other technologies.

* *Corresponding author.*
E-mail: SFriedrich@ime-aachen.de (S. Friedrich).
† These authors contributed equally to this work.

https://doi.org/10.1016/j.jmrt.2019.11.049

Please cite this article in press as: Zhang X, et al. Computation-assisted analyzing and forecasting on impurities removal behavior during zone refining of antimony. J Mater Res Technol. 2019. https://doi.org/10.1016/j.jmrt.2019.11.049

1. Introduction

High purity antimony (Sb) finds growing applications in high-tech areas, for example, Sb with a purity level of 4 N (i.e. 99.99%) is an important ingredient in Bi_2Te_3-type alloys utilized in fabricating thermoelectric coolers or power generators. Higher levels of purity (5 N) are mainly used in semiconductor industry, such as manufacturing infrared detectors, diodes and Hall Effect measuring devices in the form of AlSb, InSb as well as GaSb compounds. It is also intensively applied as n-type doping agent in germanium (Ge) and silicon (Si) semiconductors and as neutron source in nuclear reactors [1]. For the production of high purity Sb, usually commercial pure Sb or Sb_2O_3 (ca. 99.8 %) are used as starting material. Zone refining is a widely used purification technology, which operates through distributing the impurities at the crystallization interface, based on their solubility difference in solid and liquid states of metal substrate (so-called distribution coefficient, k). Zone refining has the potential to be mentioned as final-step, while talking about high-purity metals production. The distribution coefficient of every single impurity plays a key role in the final refining efficiency. The general rule is that the more deviation of k_x from unity, the more tendency impurity X shows to be segregated from the metallic substrate. However, the distribution coefficient (k) could be interpreted under (k_0) or effective distribution coefficient (k_{eff}). The equilibrium distribution coefficient (k_0) is usually regarded as constant for every single impurity, which can be attained from the known equilibrium phase diagrams. But the real crystallization process takes place always in a non-equilibrium system; therefore, the refining efficiency is indeed affected by the k_{eff}. The effective distribution coefficient (k_{eff}) is dependent on the actual experimental conditions, as it has been summarized by the so-called BPS model, developed by Burton, Prim and Slichter [2]:

$$k_{eff} = \frac{k_0}{k_0 + (1 - k_0)\, e^{-f\delta/D}} \tag{1}$$

Where, f is the crystal growth rate (assumed as moving velocity of the heater in zone melting equipment), δ is the diffusion layer thickness at the crystallization interface and D is the diffusion coefficient of each impurity in molten metal substrate. The parameters k_0 and f are known for one certain experiment in this model, hence either k_{eff} or δ/D can be calculated as the unknown parameter when one of them is determined through empirical research. This provides an alternative way to get the information of diffusion layer thickness and the diffusion coefficients of impurities in the metal. Most importantly, the acquisition of k_{eff} and δ/D is very useful to establish optimum experimental parameters and to predict the zone refining efficiency and the required time until purification target is achieved.

The research activities on zone refining of Sb were mainly conducted in 1950s–1960s [3–7]. Those researches demonstrated the effectiveness of zone refining to purify an As-free Sb. As and Pb are already known to be the most common impurities with higher contents in the commercial pure Sb and Sb_2O_3, independent from the methodology of the primary production process [8,9]. While Pb seems to be very easily removed during zone refining, As is a problematic task due to its unfavorable distribution coefficient. In order to a better understanding of the refining process and an improvement of the refining efficiency in Sb zone refining, a comprehensive knowledge on the effective distribution coefficients of impurities, the diffusion layer thickness δ as well as the diffusion coefficients of impurities (D) is extremely desirable. However, the parameters of δ as well and D in the course of Sb zone refining are still not elucidated. There is, though, a so-called "approximate graphic method", proposed by Vigdorovich, et al. [6,10] to determine the k_{eff} of impurities in Sb without consideration of δ and D. But in this method the accuracy of calculation decreases at higher number of passes, according to the same Author in another publication [11]. Hence, it can be concluded that a feasible methodology, able to precisely forecast the refining efficiency and provide optimization scheme, is not available up to now.

There is generally a variety of numerical models to describe the impurity distribution profiles, such as Lord [12] or Reiss models [13] (both based on Pfann's classic differential equations [14]), Hamming discrete model [14], Burris–Stockman–Dillon integral model [15], Spim-model [16], and Kirillov model [17], etc. Those models can be not only used to predict the zone refining efficiency, but also applied to retrieve k (one variable in the model, namely k_{eff}) by fitting the simulated data to the experimental ones. But the operability of k retrieval process and the accuracy of the results are related to the effectiveness of specific models. Lord and Reiss models are limited in the practical application, as the former does not take the normal freezing in the last zone into account and also becomes very complicated when the number of passes becomes large; the latter is only valid for impurities with values of k close to unity ($0.9 < k < 1.1$) [14]. Hamming model is the most widespread in computations, but it involves error accumulation at a large number of iterations as the molten zone is assumed to advance in discrete steps [17]. The Burris–Stockman–Dillon model is presented in integral equations. However, an analytical solution for this model has not been found, which means the numerical methods of solution have to be developed for the integration. In this case, the Burris–Stockman–Dillon model is essentially similar to the Spim-model, which is presented in a differential way, but can be easily solved with the assistance of computer. These two models are both applicable for all finite values of k and given concentration distributions over the entire length of the bar. The newly developed Kirillov model is based on the concept of the average impurity concentration in the ingot portion being refined. With the introduction of separation factor, this model is able to optimize the zone length from pass to pass. The obtained optimized zone length variation from this model is consistent with the results achieved based on Spim-model [18], while the impurity concentration profiles was not predicted through Kirillov model. Therefore, in the present work, the Spim-model was applied to derive the k_{eff} of the main impurities during zone refining process considering its high reliability and simplicity. With the help of MATLAB, the k_{eff} was obtained by fitting the concentration profile from this model to the experimental concentration profile. The k, with which the simulated concentration profile best match

Please cite this article in press as: Zhang X, et al. Computation-assisted analyzing and forecasting on impurities removal behavior during zone refining of antimony. J Mater Res Technol. 2019. https://doi.org/10.1016/j.jmrt.2019.11.049

the experimental data, is assigned to the k_{eff}. Accordingly, δ/D becomes also known based on BPS model as above mentioned. Furthermore, the k_{eff} of impurities at any given moving velocity of the heater can be calculated based on the derived δ/D and BPS model. The prediction of zone refining efficiency or impurity concentration distribution can be then realized by substituting k_{eff} into the Spim-model.

The second focus of the present work was the experimental removal of As, as its detrimental effect to zone refining of Sb is a fact. The common technologies used for this purpose – based on the state of the art – include vacuum distillation of $AsCl_3$ and $SbCl_3$ (after dissolution of Sb or Sb_2O_3 into 6 M HCl), vacuum distillation of Sb or electrolysis [19–22]. However, those technologies usually involve extra process steps, high equipment investments, increased production costs and long operational times. In order to overcome these disadvantages, an introduction of a protective gas flow during zone refining was developed in this study to reduce As by being swept away after being evaporated.

2. Experimental procedure

An industrial scale two meters long with 17 cm diameter (outer tube) horizontal zone refining equipment, provided with a single inductive heater (W 5 cm) and capable of generating up to 45 kW with 10 kHz maximum frequency was established for this work. The pieces of Sb were charged in a high purity quartz crucible boat (L 60 cm × W 5 cm), placed in a self-designed quartz (inner) tube (L 80 cm × ID 6.5 cm), which allowed the protective gas (N_2) flow from one end to the other as see in Fig. 1. This inner quartz tube was then located in the outer quartz tube before the process starts.

The initial materials for zone refining have been metallic Sb, whose chemical compositions – analyzed by ICP-OES – are represented in Table 1 and shows that the compositions of them are almost the same, except for some differences among As concentrations.

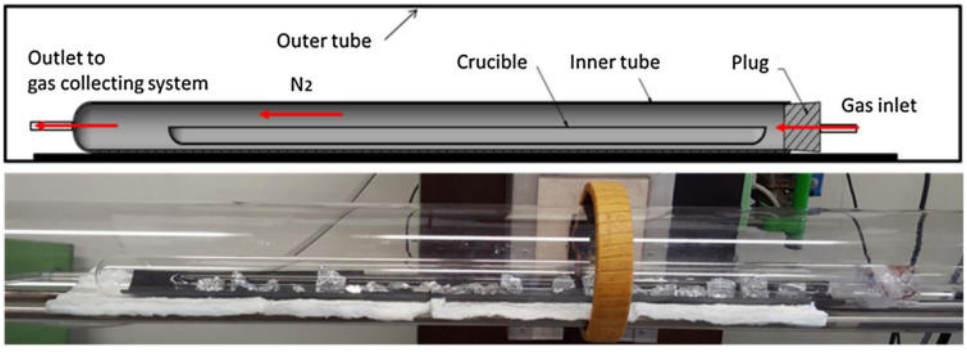

Fig. 1 – Zone refining setup.

Table 1 – Composition of initial metallic Sb material (ppm).

Code of material	As	Pb	Bi	Cu	Fe	Na	Ni	Se	Te	Zn	S	Sb (%)
a	430	1100	<10	27	84	18	15	13	<10	13	64	99.82
b	670	1100	10	30	82	<10	17	14	<10	14	67	99.80
c	380	1100	<10	27	60	16	11	12	<10	<10	64	99.83
d	480	1200	<10	22	75	13	<10	11	<10	<10	83	99.81
e	840	1300	14	44	86	<10	18	<10	<10	11	71	99.76

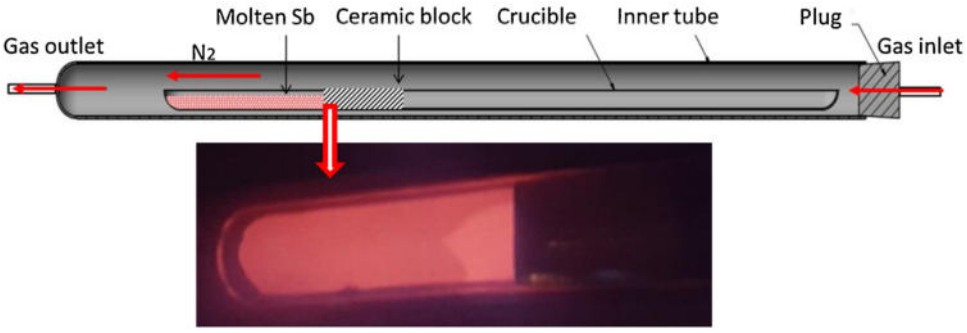

Fig. 2 – Sketch of the setup for the test on As evaporation, showing the applied ceramic block in the quartz crucible.

Please cite this article in press as: Zhang X, et al. Computation-assisted analyzing and forecasting on impurities removal behavior during zone refining of antimony. J Mater Res Technol. 2019. https://doi.org/10.1016/j.jmrt.2019.11.049

Table 2 – Experimental parameters for the test on As evaporation.

No. of experiments	Material	Time (min)				Flux rate (1 L/min, N_2)		
1	a	60	120	240	360		1	
2	b	60	120	240	360		1	
3	a		120			0.1	1	5

Table 3 – Experimental parameters of zone refining.

No. of experiments	Material	Zone length (cm)	Moving rate (mm/min)	Number of passes
4	c	15 (0.25 L)	2	2
5	d	15 (0.25 L)	1	2
6	e	15 (0.25 L)	0.5	2

2.1. *Experiments for the test on As removal by carrier gas after evaporation*

As the very first step of these investigations, the amount of As evaporation from Sb was to be examined. In order to simplify this test, only a limited sector of the crucible was brought into the focus, i.e. a ceramic block was placed in the quartz crucible to form a 15 cm long sector. In this sector, Sb was charged and melted, as seen in Fig. 2. This area is called "molten zone" and is constant for all other zone refining experiments in this paper too, represented in chapter 2.2. Thus, the As-evaporation behavior determined here will be very similar and comparable to that during practical zone refining process.

The detailed experimental parameters are listed in Table 2. As seen, the influence of carrying gas flux on As-evaporation was investigated with applying the material (a) from Table 1. Then both materials (a) and (b), including different initial As-concentrations, were used to investigate the dependency of the evaporation rate on time as well as the effect of initial concentration on the evaporation behavior. Clean and powder form samples, taken from the initial material as well as products, by drilling with clean tools, were then analyzed by ICP-OES with a lowest detection limit of 10 ppm.

2.2. *Experiments for zone refining of Sb to calculate k_{eff}*

For the tests on Sb zone refining, the setup of Fig. 1 was utilized, while each time a charge of 1.5 kg Sb was deployed in the quartz crucible. The power of inductive heating is suchlike adjusted to maintain a zone length of 15 cm (a comparatively stable molten zone under the current inductive heater), the same as mentioned in chapter 2.1. The experiments were then conducted under three different heating coil movements, each for two zone passes, while using a carrying gas flux of 1 L/min Nitrogen. The materials (c), (d) and (e) were used in this series of trial, undertaking the experimental parameters as shown in Table 3.

3. Theoretical model for simulating impurity distribution profiles after zone refining

The Spim-model is engaged in recording the impurity concentration variation in the molten zone, according to the mass conservation when assuming the molten zone moves with a displacement of dX. The details on this model can be found in reference [16], and it will not be presented here. In this model, the impurity concentration profile for each pass has been quantified by considering four different regions along the sample (see Fig. 3): Region 1, surface (X = 0); Region 2, intermediate (0 < X ≤1-Z); Region 3: normal freezing (1-Z < X < 1); and Region 4: end of the sample (X = 1) and the corresponding equation for each region is concluded in Eq. (2).

$$C^n_{S(X)} = \begin{cases} k_i\left(\frac{dx}{Z}\right)\left(\sum_{q=0}^{M-1} C^{n-1}_{S(q\,dx)}\right), & X = 0 \\ C^n_{S(X-dx)} + \frac{k_i dx}{Z}\left(C^{n-1}_{S(X+Z-dx)} - C^n_{S(X-dx)}\right), & 0 < X < 1-Z \\ \left[1+\left(\frac{1-k_i}{1-X}\right)dX\right] C^n_{S(X-dx)}, & 1-Z \le X < 1 \\ \frac{1}{dX}C_0 - \left(\sum_{X=0}^{X=1-dX} C^n_{S(X)}\right), & X = 1 \end{cases} \quad (2)$$

Where, $C^n_{S(X)}$ represents the impurity concentration at position X of the solid bar after n passes of zone refining; k_i is the effective distribution coefficient of impurity i; qdx represents the position of manually divided infinite small elements (with number of M) in the first region and C_0 is the initial concentration of impurity i.

4. Results and discussion

4.1. *Evaporatoin of As*

Due to the high vapor pressure of As in comparison to that of Sb (2.9×10^5 and 4.5×10^1 Pa for As and Sb respectively at 950 K [23]), evaporation of As during zone melting might be possible despite the fact that such condition is not considered. However, the results, as seen in Fig. 4 showed only a slight reduction for the initial As-concentration of 670 ppm by increasing melting time. Moreover, at lower concentrations, e.g. about 430 ppm, As almost cannot be removed. Besides, Fig. 4 shows a negligible reduction tendency of As at different gas flux rates, which indicates that As removal is based on evaporation from the molten Sb surface rather than depended from mass transport by a carrying gas. All results demon-

Please cite this article in press as: Zhang X, et al. Computation-assisted analyzing and forecasting on impurities removal behavior during zone refining of antimony. J Mater Res Technol. 2019. https://doi.org/10.1016/j.jmrt.2019.11.049

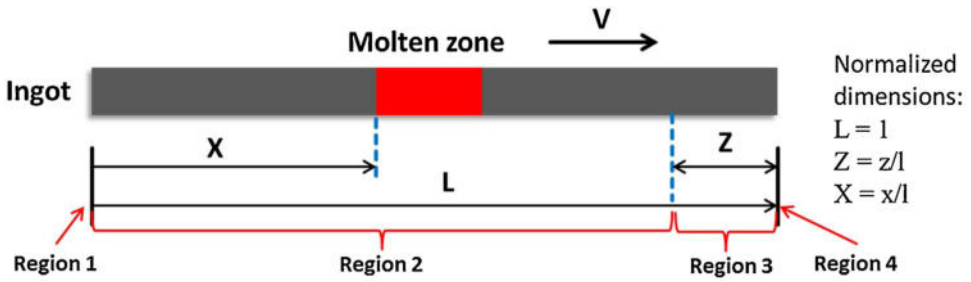

Fig. 3 – Sketch of four regions considered in Spim-model, where l, z, x are respectively the actual length of the bar, the zone length and the position of the crystallization interface, while L, Z and X are the normalized dimensions.

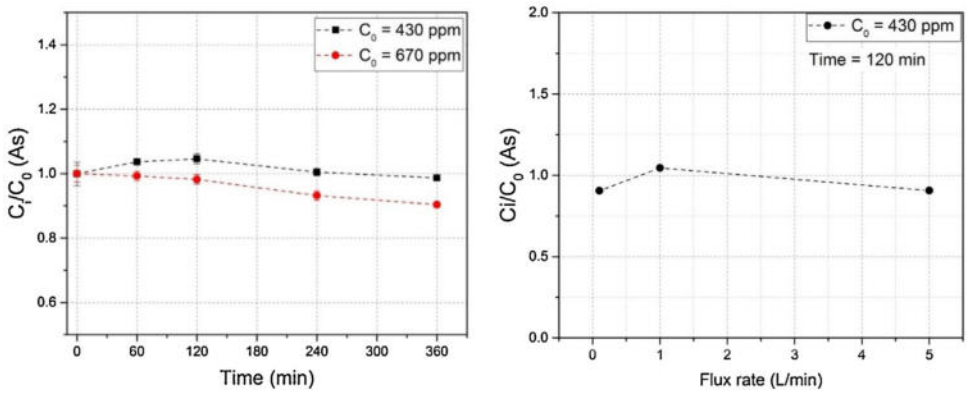

Fig. 4 – As concentration versus melting time at flux rate of 1 L/min in As evaporation measurement (left) and As concentration versus flux rate in As evaporation measurement (right).

strated the difficulty of As evaporation from a base of molten Sb when it is diluted in this substrate.

4.2. *Effective distribution coefficients of impurities*

In order to obtain the effective coefficient of one impurity, an appropriate input for the value of k into the modelling, Eq. (2), should be conducted in such a way that the simulation concentration distribution curves achieve the best matching with the experimental ones. For this "fitting" to each impurity, a variety of values for k was given to the program and the matching level was verified. The best matched k to the experimental results is then to be designated as k_{eff} for that specific impurity. In this paper, the three main impurities in Sb, i.e. Pb, As and Fe were brought into consideration. This decision was also due to the difficulty of chemical detection of other impurities with the concentrations lower than 10 ppm via ICP-OES.

4.2.1. *Lead*

Fig. 5 shows the concentration distribution of Pb along the bar and fitting with Spim-model at different induction coil movement velocities. Pb has been intensively shifted into the end of the bar with the lowest achieved Pb-concentration of nearly 1/10 of the initial concentration after one pass as well as almost 1/100 of that after two passes. Additionally, the purification effect becomes more significant when the moving velocity decreases, which is in accordance with the BPS model, Eq. (1). The fitting of all this data with the best matched simulated k at different movement velocities assessed the optimal Pb-removal from Sb with a $k_{Pb} \sim 0.08$ for two passes and at 0.5 mm/min movement velocity, as it has the lowest k-value among the tested conditions.

Using the simulation via Spim-model can give some good hints about the highest reasonable number of passes at a specific velocity to achieve a satisfying high level of purification effect. Fig. 6 represents a relationship between different numbers of passes as well as different heater movement velocities (both together defining the total time effort of the process) and their effect on the average of refining (the k_{eff} for 0.1 mm/min was theoretically calculated based on BPS model). It can be seen that the Pb refining efficiency after each single pass decreases as zone pass increases. The highest refining efficiency, i.e. the lowest average C_S/C_0, is achieved, when the zone passes are over six. This tendency is irrespective of the heater moving velocity. However, the lower velocity leads to a higher maximum refining efficiency. When aiming to introduce a zone refining process in the shortest possible time, a combination of different situations of movement velocity as well as number of passes has to be considered. For example, in order to achieve an exemplary Pb-removal up to $C_0/1000$, either a heating coil velocity of 0.1 or 0.5 mm/min under 4 passes or a velocity of 1.0 mm/min under 5 passes should be employed (see Fig. 6). Obviously, using 1.0 mm/min is more favorable than the others considering much less time consumed in one single pass.

Please cite this article in press as: Zhang X, et al. Computation-assisted analyzing and forecasting on impurities removal behavior during zone refining of antimony. J Mater Res Technol. 2019. https://doi.org/10.1016/j.jmrt.2019.11.049

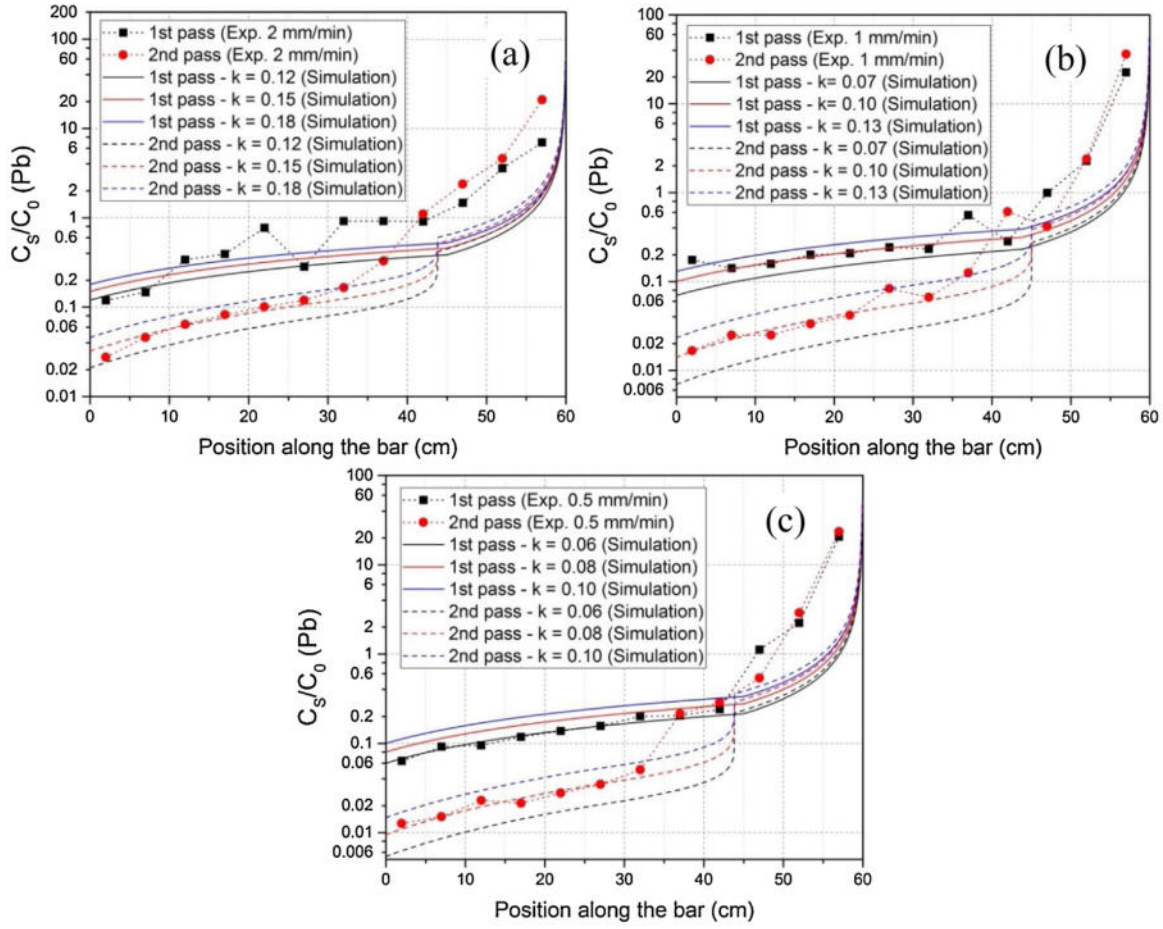

Fig. 5 – Concentration distribution of Pb along the bar and fitting with Spim-model at different induction coil movement velocities: (a) 2 mm/min, (b) 1 mm/min, and (c) 0.5 mm/min.

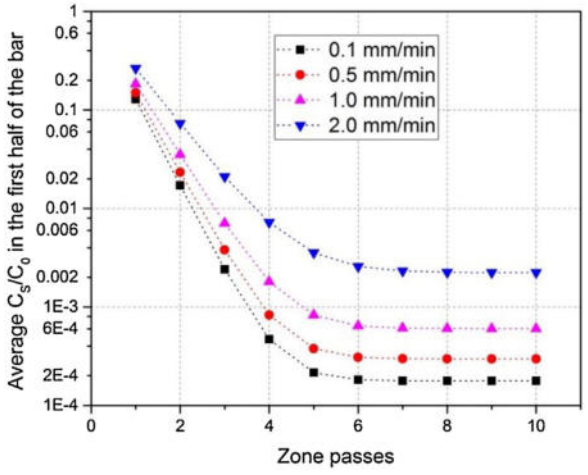

Fig. 6 – Remaining average Pb concentrations in the first half of the bar against zone passes under different movement velocities of the heater.

4.2.2. *Arsenic*

In contrast to Pb, As is quite difficult to be removed via zone refining process, as seen in Fig. 7 with huge difference to that of Fig. 5. The values of k_{As} – even at the lowest movement velocity – is still much higher than that of Pb at the highest velocity, A negligible removal of only 20–30% in the first 20 cm of the bar takes place after two passes at both velocities of 2 as well as 1 mm/min. By decreasing the moving rate to 0.5 mm/min, a considerable As removal of about 40–60% occur after two passes (see Fig. 7c). This value however, is lower than that of Pb-removal under the same experimental conditions.

Similar to Pb, the varied simulation-based concentration distribution profiles were fitted to that of experimental ones. It was observed that the calculated value for k_{eff} at 0.5 mm/min moving rate is much lower than k_0 ($k_{0,As} \sim 0.64$ [20]), although the experimental k_{eff} should be always bigger than the theoretical k_0. Noticing the fact that the initial As-concentrations have not been consistent in this series of experiments (initial concentrations of 380, 480 and 840 ppm for experiments of 2, 1 and respectively 0.5 mm/min were applied). Considering the results mentioned in chapter 4.1 about the negligible As evaporation at lower concentrations, but considerable evaporation at higher concentrations, the unexpected low value of k_{eff} at 0.5 mm/min can be interpreted as a consequence of not only fractional crystallization but also an overlapping evaporation effect. In order to separate both effects by introducing a "correction-factor" to this value and thus make it closer to

Please cite this article in press as: Zhang X, et al. Computation-assisted analyzing and forecasting on impurities removal behavior during zone refining of antimony. J Mater Res Technol. 2019. https://doi.org/10.1016/j.jmrt.2019.11.049

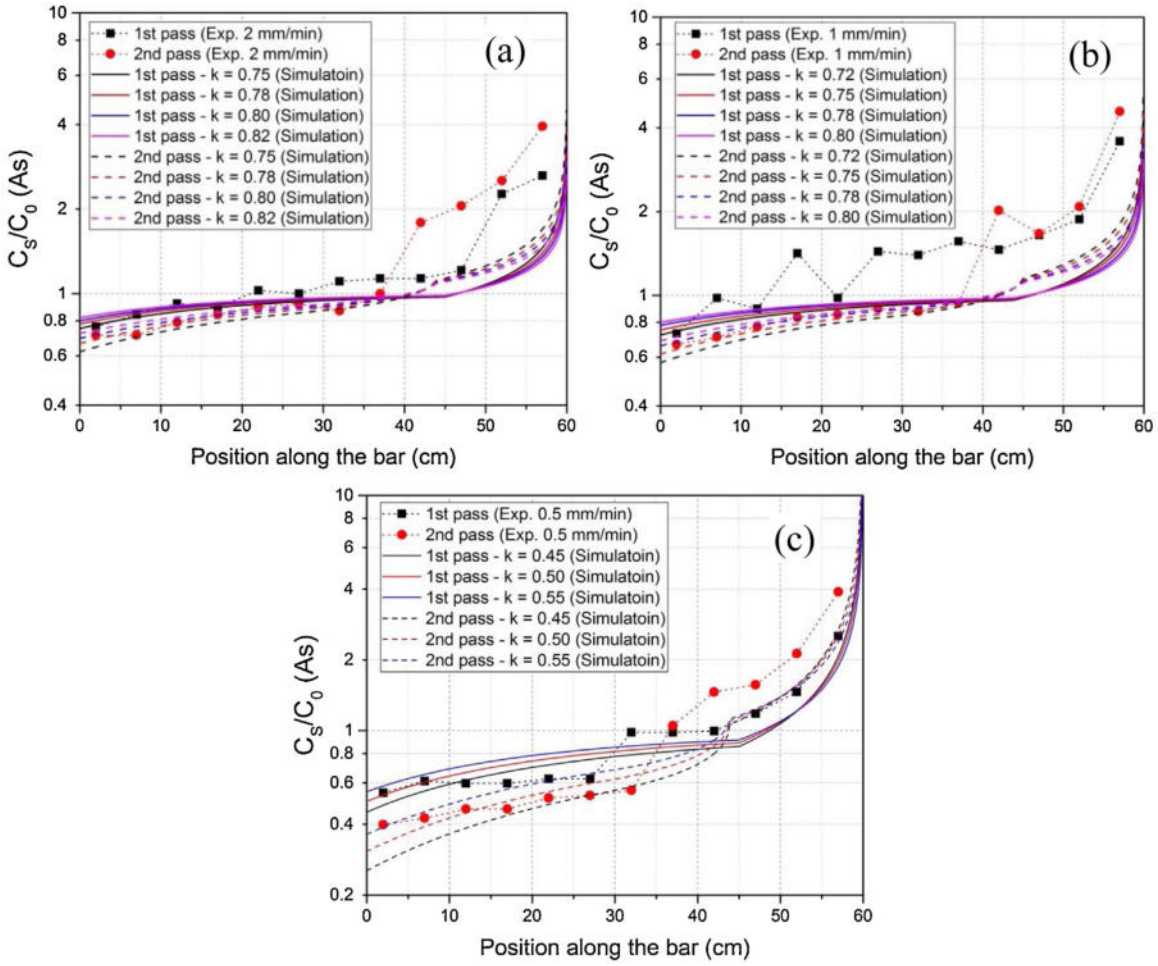

Fig. 7 – As concentration distribution and fitting with Spim-model: (a) 2 mm/min, (b) 1 mm/min and (c) 0.5 mm/min, in which (c) is the corrected version using 90% of the initial concentration.

that of crystallization theory, the initial As concentration was considered as 90% of 840 ppm, because according to Fig. 4, almost 10% As will be evaporated under these experimental conditions. However, the derived k_{eff} after this correction, i.e. approx. 0.5 as seen in Fig. 7(c), is still lower than the equilibrium distribution coefficient k_0. Unfortunately, an evaporation factor cannot be taken into account in Spim-model, as it falsifies the results. This is the shortcoming of the simulation in the case of As, but only at higher initial concentrations because its evaporation at concentrations lower than around 430 ppm is negligible. A solution for this problem could be an updated model enabling to import an evaporation coefficient regarding to the volatile impurities to derive a more precise result, but it is out of the scope of this paper.

4.2.3. *Iron*

The Fe-contamination is significantly lower than that of Pb and As, though with the content of around 80 ppm it is still the third main impurity in commercial Sb. Fig. 8 shows that it can be considerably removed by zone refining, i.e. almost above 80 % Fe-removal in the first half of the bar, leading to be reduced to amounts lower than 10 ppm just after one pass of zone refining at 0.5 mm/min moving rate. Similar to the two other investigated impurities, the values of k_{eff} were obtained for different heating coil movement velocities using Spim-model-based simulation. Here, the k_{eff} values of 0.3 as well as 0.2 were attained for the rates of 2 and 1 mm/min respectively. For the case of 0.5 mm/min moving rate, no precise k_{eff} could be calculated due to the previously mentioned analytical limit of ICP-OES (10 ppm). But the k_{eff} at this rate should be smaller than 0.12 (10 ppm/80 ppm).

Based on the above mentioned trials and results, the k_{eff} for the investigated impurities Pb, As and Fe at different heating coil movement velocities are summarized in Table 4. The sequence of degree in impurity removal from Sb via zone refining methodology can be observed in this table as Pb < Fe < As. The k_{eff} of Pb at 2 mm/min under the present experimental system corresponds well to the k_{eff} retrieved by "approximate graphic method" in the literature [6], though the experimental conditions differ from each other (quartz crucible and induction heater used in the present work, graphite crucible and resistance heater under magnetic agitation for the other). The

Please cite this article in press as: Zhang X, et al. Computation-assisted analyzing and forecasting on impurities removal behavior during zone refining of antimony. J Mater Res Technol. 2019. https://doi.org/10.1016/j.jmrt.2019.11.049

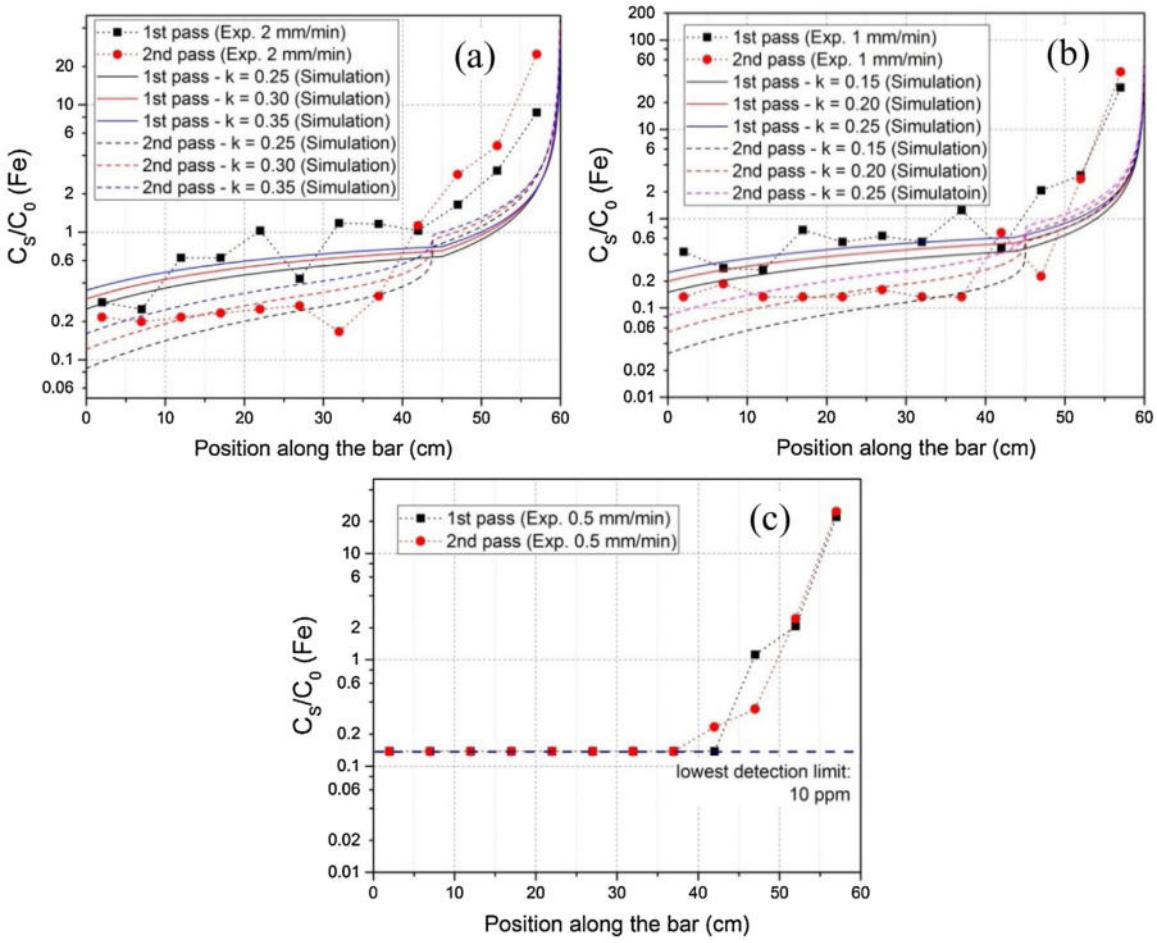

Fig. 8 – Fe concentration distribution and fitting with Spim-model: (a) 2 mm/min, (b) 1 mm/min and (c) 0.5 mm/min, in which a simulation-based fitting for (c) was not possible due to the lack of analytics.

Table 4 – Spim-model-based values of k_{eff} of Pb, As and Fe at different heater moving rate and the comparison with the results from the literature [6,24].

Impurity	Moving rate of heater (mm/min)	Average C_S/C_0 after two passes (in first half of the bar)	k_{eff}	$\ln\left(\frac{1-k_{eff}}{k_{eff}}\right)$	k_{eff} with magnetic agitation [6]	k_{eff} without magnetic agitation [6,24]
	2	0.087	0.15	1.73	0.10	0.33
Pb	1	0.042	0.10	2.20	–	–
	0.5	0.026	0.08	2.44	–	–
	2	0.820	0.80	−1.39	–	0.80
As	1	0.801	0.75	−1.10	–	–
	0.5	0.480	0.50	0.00	–	–
	2	0.220	0.30	0.85	–	0.10
Fe	1	0.145	0.20	1.39	–	–
	0.5	0.138	<0.12	>1.99	–	–

investigated k_{eff} of Pb seems to be lower than the value derived in [6,24], which is reasonable considering the absence of magnetic agitation in the molten zone in those works. However, the k_{eff} of As and Fe are deviated from expectation, i.e. not less than the values in the works without magnetic agitation, which could be resulted from the difference of ways to obtain k_{eff} and the discrepancy of experimental conditions except for heater (e.g. crucible, size of charge, ways of cooling, etc.). In addition, the value of the item $\ln\left(\frac{1-k_{eff}}{k_{eff}}\right)$ was calculated and represented in this table too, in order to be applied in BPS model in next chapter.

4.3. *Application of BPS model*

Not only forecasting the zone refining effect for each impurity at different experimental conditions can be realized through Spim-model-based simulation, but also the obtained k_{eff} can

Please cite this article in press as: Zhang X, et al. Computation-assisted analyzing and forecasting on impurities removal behavior during zone refining of antimony. J Mater Res Technol. 2019. https://doi.org/10.1016/j.jmrt.2019.11.049

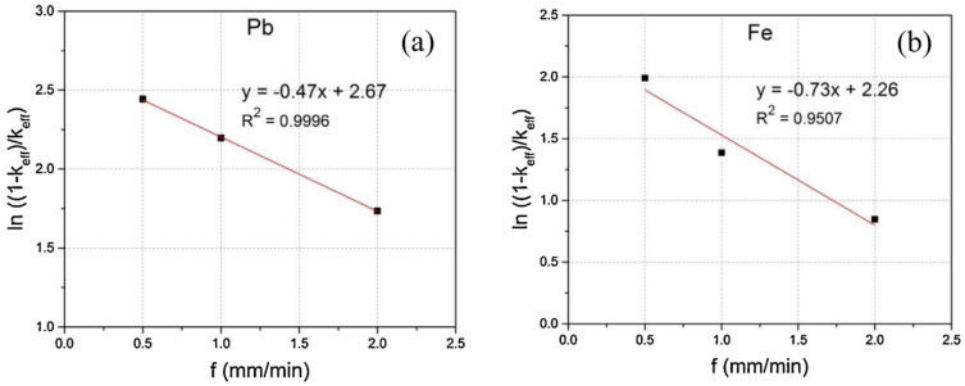

Fig. 9 – The relation between ln $\left(\frac{1-k_{eff}}{k_{eff}}\right)$ versus moving velocity of heater (f) for impurities of Pb and Fe.

Table 5 – δ/D and k_0 for Pb and Fe.

Impurity	δ/D	ln $\left(\frac{1-k_0}{k_0}\right)$	k_0	k_0 in reference [20]	k_0 from Factsage
Pb	0.47	2.67	0.06	0.06	0.05
Fe	0.73	2.26	0.09	0.03	«0.01

be taken into account in the BPS model, Eq. (1), after transforming it into another form as shown in Eq. (3) [25–27]:

$$\ln\left(\frac{1-k_{eff}}{k_{eff}}\right) = \ln\left(\frac{1-k_0}{k_0}\right) - f\frac{\delta}{D} \quad (3)$$

This allows to obtain the ratio of δ/D from Eq. (3), which represents to some extent the purification potential and is very difficult to be determined experimentally or assumed theoretically. It can be seen in Eq. (3) that the item of ln $\left(\frac{1-k_{eff}}{k_{eff}}\right)$ has a linear relationship with the heating coil movement velocity, in which δ/D and k_0 are taken from the slops as well as the intercepts respectively. Based on the data in Table 4, the linear relationship between ln $\left(\frac{1-k_{eff}}{k_{eff}}\right)$ and f for each impurity are illustrated as in Fig. 9. As was not taken into account for the linear fitting as the k_{eff} at moving rate of 0.5 mm/min is inaccurate resulted from the evaporation. It is not meaningful to fit linear relationship with two points. In the case of Fe and for the rate of 0.5 mm/min, k_{eff} = 0.12 was assumed. With derivation of intercepts and slops in the diagram, the mathematical values for δ/D as well as k_0 were calculated for each and represented in Table 5. It shows the absolute similarity between the empirical obtained k_0 and the one extracted from the literatures [20] and/or calculated in the thermochemical software FactSage. That confirms the effectiveness of the applied methodology and its process window. The diffusion layer thickness δ or diffusion coefficients D for each impurity would be easily retrieved when one of them is known.

5. Conclusions

Impurity removal behavior and prediction of their purification effects in commercial pure Sb have been investigated with the assistance of numerical simulation in this work. As evaporation behavior was firstly investigated under different inert gas flow rate and melting time. The results showed that As-concentration with higher initial values such as 670 ppm can be removed via evaporation, but just slightly, as the melting time increases (e.g. 10 % reduction while the melting time is 360 min). However, in the case of lower initial concentrations of As, it did not show any reduction at different gas fluxes or melting times. It confirms the fact, that As impurity must be removed via a separated vacuum distillation or chemical ways before applying in the zone refining process.

In the second part of the investigations, zone melting process to refine Sb was conducted under inert gas flux and the heater moving rates of 2, 1 as well as 0.5 mm/min. Using a simulation based on the so-called Spim-model, the values of k_{eff} for the impurities of Pb, As and Fe at each moving rate were retrieved by fitting the experimentally achieved impurity concentration profiles with that through Spim-model. That helps to more precisely predict the required zone passes, time and the achieved refining efficiency for Sb-zone melting. In addition, based on BPS model, the equilibrium distribution coefficients for each impurity were calculated, showing the accordance with the theoretical data and therefore confirming the effectiveness of the selected methodology. Finally, an almost unknown but important parameter, the ratio of diffusion layer thickness to diffusion coefficient (δ/D), was obtained too, based on BPS model. That not only allows to predict k_{eff} for any moving velocity based on Spim-model, but also provides an alternative way to calculate these two values when one of them was obtained from other technologies.

Author contributions

Bernd Friedrich was the principal investigator. Semiramis Friedrich and Xiaoxin Zhang conceived and designed the experiments. Bin Liu performed the experiments. Xiaoxin Zhang and Semiramis Friedrich analyzed the data. Xiaoxin Zhang and Tianxiang Huang conducted the simulation.

Please cite this article in press as: Zhang X, et al. Computation-assisted analyzing and forecasting on impurities removal behavior during zone refining of antimony. J Mater Res Technol. 2019. https://doi.org/10.1016/j.jmrt.2019.11.049

Xiaoxin Zhang and Semiramis Friedrich wrote and edited the manuscript. Bernd Friedrich edited the manuscript finally.

Conflicts of interest

The authors declare no conflicts of interest.

Acknowledgments

The authors would like to thank CSC - China Scholarship Council for the financial support of the PhD candidate Mr. Xiaoxin Zhang.

REFERENCES

[1] Anderson C. SME mineral processing and extractive metallurgy handbook (Antimony production and commodites). Trans Soc Min Metall Explor Inc 2019.
[2] Burton JA, Prim RC, Slichter WP. The distribution of Solute in crystals grown from the melt. Part I. Theoretical. J Chem Phys 1953;21:1987, http://dx.doi.org/10.1063/1.1698728.
[3] Tanenbaum M, Goss AJ, Pfann WG. Purification of Antimony and tin by a new method of zone refining. J Met 1954;6:762–3.
[4] Kro' LYa, Ivleva VS. Preparation of high-purity Antmony by zone melting. Moscow: Metallurgizdat; 1959.
[5] Vigdorovich VN, Ivleva VS, Krol LY. Purification of Antimony by zone recrystallization. Russ Metall Fuels 1960:29–33.
[6] Vigdorovich VN, Ivleva VS. A method of approximate graphical determination of effective coefficients of distribution in zone refining. Russ Metall Fuels 1960:57–63.
[7] Huntley DA, Shah JS. High resistance ratio antimony. J Cryst Growth 1970;6:216–8.
[8] Anderson CG. The metallurgy of antimony. Chemie Der Erde - Geochem 2012;72:3–8, http://dx.doi.org/10.1016/j.chemer.2012.04.001.
[9] Dupont D, Arnout S, Jones PT, Binnemans K. Antimony recovery from end-of-Life products and industrial process residues: a critical review. J Sustain Metall 2016;2:79–103, http://dx.doi.org/10.1007/s40831-016-0043-y.
[10] Vigdorovich VN. Purification of metals and semiconductors by crystallization. Moscow: Freund Publishing Houste; 1969.
[11] Vigdorovich VN, Rozin KM. On procedures for determing the effective distribution coefficients during zone refining. Russ Metall Fuels 1962:25–9.
[12] Lord NW. Trans AIME; 1953. p. 1531.
[13] Reiss H. Mathematical methods for zone-melting processes. J Miner Met Mater Soc 1954;6:1053–9.
[14] Pfann WG. Zone melting. 2nd ed. New York: John Wiley and Sons. Inc; 1966.
[15] Burris L Jr, Stockman CH, Dillon IG. Contribution to mathematics of zone refining. J Miner Met Mater Soc 1955;7:1017–23.
[16] Spim JA, Bernadou MJS, Garcia A. Numerical modeling and optimization of zone refining. J Alloys Compd 2000;298:299–305, http://dx.doi.org/10.1016/S0925-8388(99)00655-6.
[17] Kirillov YP, Churbanov MF. Zone recrystallization modeling and optimization based on the concept of average impurity concentration in the ingot portion being refined. Inorg Mater Appl Res 2016;52:201–6, http://dx.doi.org/10.1134/S0020168516010106.
[18] Ghosh K, Mani VN, Dhar S. Numerical study and experimental investigation of zone refining in ultra-high purification of gallium and its use in the growth of GaAs epitaxial layers. J Cryst Growth 2009;311:1521–8, http://dx.doi.org/10.1016/j.jcrysgro.2009.01.102.
[19] Singh AJ, Mathur BS, Suryanarayana P. Preparation of electronics grade bismuth, antimony, tellurium, cadmium and zinc by vacuum distillation and zone refining; 1975.
[20] Huang Z. Investigation of vacuum purification of Sb and production of high purity Sb. Kunming University of Science and Technology; 2003.
[21] Jevtic D, Vitorovic D. A new procedure for the preparation of antimony of high purity combined with the production of antimony trioxide of high purity. Ind Eng Chem Prod Res Develop 1974;13:275–9, http://dx.doi.org/10.1021/i360052a012.
[22] Iyer RK, Deshpande SG. Preparation of high-purity antimony by electrodeposition. J Appl Electrochem 1987;17:936–40, http://dx.doi.org/10.1007/BF01024359.
[23] Kong XF, Yang B, Xiong H, Kong LX, Liu DC, Xu BQ. Thermodynamics of removing impurities from crude lead by vacuum distillation refining. Trans Nonferrous Met Soc China (English Ed) 2014;24:1946–50, http://dx.doi.org/10.1016/S1003-6326(14)63275-1.
[24] Vigdorovich VN, Ivleva VS, Krol' LYa. Refining antimony by the zone-crystallization method. Izv Akad Nauk SSSR. Metall I Topl 1960:44–9.
[25] Johnston WC, Tiller WA. Fluid flow control during solidification. Part I. Trans AIME 1961;221:331–6.
[26] Ostrogorsky AG, Müller G. A model of effective segregation coefficient, accounting for convection in the solute layer at the growth interface. J Cryst Growth 1992;121:587–98, http://dx.doi.org/10.1016/0022-0248(92)90566-2.
[27] Hu S, Nozawa J, Koizumi H, Fujiwara K, Uda S. Grain boundary segregation of impurities during polycrystalline colloidal crystallization. Cryst Growth Des 2015;15:5685–92, http://dx.doi.org/10.1021/acs.cgd.5b00646.

Please cite this article in press as: Zhang X, et al. Computation-assisted analyzing and forecasting on impurities removal behavior during zone refining of antimony. J Mater Res Technol. 2019. https://doi.org/10.1016/j.jmrt.2019.11.049